**Biogeosciences
Discussions**

Biogeosciences Discussions is the access reviewed discussion forum of *Biogeosciences*

BGD

4, 1737–1777, 2007

Sea surface CO$_2$
fugacity in the
subpolar North
Atlantic

A. Olsen et al.

The sea surface CO$_2$ fugacity and its relationship with environmental parameters in the subpolar North Atlantic 2005

A. Olsen[1,2,3]**, K. R. Brown**[1]**, M. Chierici**[3]**, T. Johannessen**[2,1]**, and C. Neill**[1]

[1]Bjerknes Centre for Climate Research, University of Bergen, Bergen, Norway
[2]Geophysical Institute, University of Bergen, Bergen, Norway
[3]Marine Chemistry, Department of Chemistry, Göteborg University, Göteborg, Sweden

Correspondence to: A. Olsen (are.olsen@gfi.uib.no)

Title Page

Abstract	Introduction
Conclusions	References
Tables	Figures

|◄ | ►|

◄ | ►

Back | Close

Full Screen / Esc

Printer-friendly Version

Interactive Discussion

EGU

Abstract

We present the first year-long subpolar transatlantic set of surface seawater CO_2 fugacity ($f\mathrm{CO}_2^{sw}$) data. The data were obtained aboard the MV *Nuka Arctica* in 2005 and provide a quasi-continuous picture of the $f\mathrm{CO}_2^{sw}$ variability between Denmark and

5   Greenland. Complementary real-time high resolution data of surface chlorophyll *a* (chl *a*) concentrations and mixed layer depth (MLD) estimates have been collocated with the $f\mathrm{CO}_2^{sw}$ data. Off the shelves the $f\mathrm{CO}_2^{sw}$ goes through a pronounced seasonal cycle. Surface waters are saturated to slightly supersaturated over a wide range of temperatures in winter. Through spring and summer $f\mathrm{CO}_2^{sw}$ decreases by approximately

10   60 μatm due to biological carbon consumption which is not fully counteracted by the $f\mathrm{CO}_2^{sw}$ increase due to summer warming. The changes are synchronous with changes in chl *a* concentrations and MLD, and $f\mathrm{CO}_2^{sw}$ is correlated to both of these through exponential decay and growth curves, respectively. In particular, MLD appears to be able to predict open ocean subpolar $f\mathrm{CO}_2^{sw}$ to within 12 μatm using a single equation for

15   the whole year. The predictive capability of chl *a* is around 20% less, with root mean square values of 14.5 μatm. As $f\mathrm{CO}_2^{sw}$ extrapolation parameters, both MLD and chl *a* outperform sea surface temperatures in the open subpolar North Atlantic. However, the situation on the shelves is much more heterogeneous and the $f\mathrm{CO}_2^{sw}$–parameter relationships are not as strong as they are off the shelves.

20   ## 1   Introduction

The rise in atmospheric CO_2 concentrations from man-made sources and resultant climate change is mitigated in part by oceanic carbon uptake. During the 1990s the annual uptake corresponded to roughly one quarter of annual emissions (Prentice et al., 2001). The extent to which this uptake will be sustained in the future is an open

25   question incurring uncertainties in projections of climate change. Arrival at the required state of knowledge can be accelerated through continued observations of the

ocean carbon cycle over regions and time periods of sufficient extent to resolve and understand current large-scale and long-term changes. The international ocean CO_2 research community has responded with a coordinated research effort to ensure collection of the required data in all ocean basins. This includes both snapshots of interior ocean carbon chemistry, like those collected during the WOCE/JGOFS global CO_2 survey (Wallace, 2001) and continued through for instance the U.S. CO_2/CLIVAR Repeat Hydrography and the EU IP CARBOOCEAN, and quasi-continuous observations of the surface ocean CO_2 fugacity (fCO_2^{sw}) through for instance the EU IP CARBOOCEAN. The surface observations are mostly collected by autonomous instruments carried by a network of commercial vessels, Voluntary Observing Ships (VOS), and results have so far been presented on the annual surface ocean carbon cycle in the North Pacific (Chierici et al., 2006), midlatitude North Atlantic (Lüger et al., 2004), subtropical North Atlantic (Cooper et al., 1998), and Caribbean Sea (Olsen et al., 2004; Wanninkhof et al., 2007). This paper presents the first set of fCO_2^{sw} data covering a full annual cycle obtained on the northernmost VOS in the Atlantic Ocean, the MV *Nuka Arctica*, which crosses between Denmark and Greenland at approximately 60° N.

The North Atlantic is one of the more important CO_2 uptake regions of the world's oceans due to the cooling of waters travelling northward as the upper limb of the meridional overturning circulation and extensive biological activity. Indeed, data from the midlatitude regions show that surface waters are undersaturated throughout the year except for in the western parts where the waters are supersaturated in summer (Lüger et al., 2004). From the northern reaches, on the other hand, the amount of published data describing a full annual cycle are limited. In fact, as far as we are aware, the only published results are from the repeated visits from 1983 through 1991 to four stations located around Iceland (Takahashi et al., 1993) and the data from SURATLANT (Corbiere et al., 2007). However, these are both only from the western regions of the northern North Atlantic and the latter have been calculated from shore-based analyses of total alkalinity (At) and dissolved inorganic carbon (Ct), making the absolute values of fCO_2^{sw} uncertain.

Given the importance of the marine carbon cycle ascribed to the northern North Atlantic a detailed description is overdue. This is provided here using data obtained aboard *Nuka*. Unfortunately, scientists are not allowed to travel aboard *Nuka* so sampling possibilities for other biogeochemical parameters are limited. To overcome this,

5 we have taken advantage of international remote sensing and data assimilation capabilities and use remotely sensed chlorophyll *a* (chl *a*) from the Sea-viewing Wide Field-of-view Sensor (SeaWiFS) that have been collocated with the *Nuka* $f\mathrm{CO}_2^{sw}$ data. We also present collocated sea surface salinity (SSS) and mixed layer depth (MLD) data from the Forecasting Ocean Assimilation Model (FOAM) of the U.K. National Centre

10 for Ocean Forecasting (McCulloch et al., 2004).

Moreover, similar to efforts in the North Pacific (Chierici et al., 2006), midlatitude North Atlantic (Lüger et al., 2004) and tropical Atlantic (Lefévre et al., 1994), we provide explicit estimates of the importance of the different processes that drive $f\mathrm{CO}_2^{sw}$ variability in the subpolar North Atlantic. Specifically, we determine the magnitude of

15 the change in $f\mathrm{CO}_2^{sw}$ that is to be expected from gas exchange, changes in temperature, and from biology and mixing during each month. We also use salinity values to estimate the effects of concentration and dilution of Ct and At on $f\mathrm{CO}_2^{sw}$. This has been shown to be significant in the Caribbean Sea (Wanninkhof et al., 2007).

The ultimate goal of the global $f\mathrm{CO}_2^{sw}$ observation effort is to constrain regional

20 ocean carbon uptake on seasonal to interannual timescales. If this is to be achieved through ocean observations alone, significant investments of time and money are required. Moreover, instrument failure and availability of ships will inevitably restrict sampling coverage. The costs involved can be significantly reduced by using data provided by space-borne sensors with near synoptic global coverage as extrapolation parame-

25 ters for $f\mathrm{CO}_2^{sw}$; the feasibility of which has been demonstrated using SST in regions like the North Pacific (Stephens et al., 1995), Equatorial Pacific (Boutin et al., 1999; Cosca et al., 2003), and Sargasso and Caribbean Seas (Nelson et al., 2001; Olsen et al., 2004). In the North Atlantic the use of SST has not been very successful, particularly in summer (Olsen et al., 2003). Other variables such as chl *a* have been suggested

Sea surface CO$_2$ fugacity in the subpolar North Atlantic

A. Olsen et al.

Title Page

Abstract	Introduction
Conclusions	References
Tables	Figures

|◄ | ►|

◄ | ►

Back | Close

Full Screen / Esc

Printer-friendly Version

Interactive Discussion

but either no relationships have been found (Lüger et al., 2004; Nakaoa et al., 2006) or else they are only valid on short spatial scales (Watson et al., 1991). Recently MLD has, in combination with SST and position information in multilinear regressions, been introduced as an $f\mathrm{CO}_2^{sw}$ extrapolation parameter by Lüger et al. (submitted to JMS).

5 We use the *Nuka* data, with their high frequency and annual coverage, as an opportunity to track down any relationships that may exist in the subpolar North Atlantic. Here we will only deal with $f\mathrm{CO}_2^{sw}$ -parameter relationships. Multilinear regressions and flux calculations will be the focus of Chierici et al. (2007)[1].

2 Methods

10 ### 2.1 Hydrographic setting

The hydrographic conditions along the track of *Nuka* are best illustrated through a section of SSS and bathymetry as shown in Fig. 1. A map of the major surface currents is presented in Fig. 2. The North Sea is a shallow coastal ocean with a sharp salinity gradient at approximately 5° E. To the west of this all waters are basically derivatives

15 of the North Atlantic Current, NAC, frequently referred to as Subpolar Mode Waters (SPMW) (McCartney and Talley, 1982). The SPMW circulate westward, progressively cooling and freshening and branching off to the Nordic Seas. The SPMW end up in the Labrador Sea and mix with waters of polar origin, forming Subarctic Intermediate Water (SAIW). This spreads east and north and, while feeding back in on the SMPW, con-

20 stitutes a fresh and cold end member for this water mass (Lacan and Jeandel, 2004; Pollard et al., 2004). In accordance with this, the most saline waters are found over the Hatton Trough and Plateau (Fig. 1) and these stem more or less directly from the NAC and the Continental Slope Current (CSC) (Hansen and Østerhus, 2000). Surface

---

[1]Chierici, M., Olsen, A., Triñanes, J., and Wanninkhof, R.: Algorithms to estimate carbon dioxide in the upper subarctic North Atlantic using ship observations in combination with satellite and model data, Deep-Sea Res., in preparation, 2007.

Sea surface CO2 fugacity in the subpolar North Atlantic

A. Olsen et al.

waters in the Iceland Basin are fresher and mostly homogenous as a result of recirculation in the area. The interior of the Irminger Sea is dominated by SAIW, and the rim by SPMW which loops around the basin as recognised in the slight peak in salinity over the East Greenland Shelf Edge. To the far west is the East Greenland Current,

5 carrying ice and low salinity waters from the Arctic Ocean southwards.

2.2 $f\mathrm{CO}_2^{sw}$ measurements

The container carrier MV *Nuka Arctica* is operated by Royal Arctic Lines of Denmark. The ship crosses the Atlantic at roughly 60° N in about five days, depending on the weather. Between the crossings, approximately one week is spent along the west coast

10 of Greenland and three days in Aalborg, Denmark. The $f\mathrm{CO}_2^{sw}$ system was installed on board during 2004. The data discussed here are from 2005, the first year a full annual cycle was covered. They can be obtained from the Carbon Dioxide Information Analysis Centre (CDIAC) at http://cdiac.esd.ornl.gov/oceans/home.html.

The $f\mathrm{CO}_2^{sw}$ instrument installed aboard *Nuka* analyzes the CO_2 concentration in an

15 air headspace in equilibration with a continuous stream of seawater using a LI-COR 6262 non-dispersive infrared (NDIR) CO_2/H_2O gas analyzer, and is a modified version of instruments described by Feely et al. (1998) and Wanninkhof and Thoning (1993). The main modifications are a smaller equilibrator and the method of drying the headspace air. Whereas the equilibrator in the referenced systems had a volume of

20 24 l, the equilibrator on *Nuka* has a volume of approximately 1.5 l. It is vented to the atmosphere via a smaller equilibrator to pre-equilibrate the vent air. The equilibrator headspace air is circulated at 70 ml min^{-1} through a Permapure Naphion dryer to the NDIR and then returned to the equilibrator. The NDIR is run in absolute mode. Equilibrator headspace samples are analysed every 2.5 min and the instrument is calibrated

25 every 5th hour with three reference gases with approximate concentrations of 200 ppm, 350 ppm, and 430 ppm traceable to reference standards provided by NOAA/Earth System Research Laboratory. The NDIR is zeroed and spanned once a day using a CO_2-free gas and the high standard, respectively.

Title Page

Abstract | Introduction

Conclusions | References

Tables | Figures

◄ | ►

◄ | ►

Back | Close

Full Screen / Esc

Printer-friendly Version

Interactive Discussion

EGU

For our analysis the raw dry xCO$_2$ values reported by the NDIR were standardised using a linear fit between measured concentrations of the CO$_2$ standards and the off-sets from calibrated values. Equilibrator CO$_2$ fugacity was calculated from the mole fraction as described by Feely et al. (1998) and Wanninkhof and Thoning (1993):

$$f\text{CO}_2^{eq} = x\text{CO}_2(p^{\text{eq}} - p\text{H}_2\text{O})e^{p^{eq}\frac{B+2\delta}{\text{RT}_{eq}}} \tag{1}$$

where p^{eq} is the pressure of equilibration, $p\text{H}_2\text{O}$ is the water vapour pressure (Weiss and Price, 1980), R is the gas constant, and B and δ are the first and cross virial coefficients (Weiss, 1974). Sea surface CO$_2$ fugacity, $f\text{CO}_2^{\text{sw}}$, was obtained by employing the thermodynamical fCO$_2$ temperature dependence of Takahashi et al. (1993) to correct for the roughly 0.5°C difference between intake and equilibrator temperatures, with the latter being warmer.

In 2005 the instrument was installed in the bow and water was drawn from an intake at approximately 2 m depth. In bad weather the intake breached the surface, and the instrument was shut down on these occasions. Moreover, it was not possible to draw an air line from the bow down to the instrument for measurement of ambient marine air as is routinely done on such installations. The atmospheric CO$_2$ data used here were obtained from the Climate Monitoring Division of NOAA/Earth System Research Laboratory (http://www.cmdl.noaa.gov/). Data of monthly mean mole fraction collected from Storhofdi, Vestmannaeyjar, Iceland (63.3° N) and Mace Head, Ireland (53.3° N) were linearly regressed to obtain the equations describing the latitudinal gradient of monthly mean xCO$_2$. Using these equations an atmospheric xCO$_2$ value was determined for each $f\text{CO}_2^{\text{sw}}$ sample point. The mole fractions were converted to atmospheric CO$_2$ fugacity, $f\text{CO}_2^{\text{atm}}$, using Eq. (1) with the exception that SST was used in place of T_{eq}.

In 2005, data were obtained on 27 of 30 crossings of the Atlantic, starting 7 January and ending 3 December when the ship went on a five month charter in the Baltic. More than 46 000 measurements were obtained and the positions of all data are shown in Fig. 3; most of them have been obtained along approximately 60° N. The ship did a port call in Reykjavik on four occasions, hence the occurrence of a few more northerly

routes.

2.3 Remotely sensed data

Surface ocean chl *a* data derived from radiation measurements of the SeaWiFS instrument carried aboard the SeaStar (ORBVIEW-2) spacecraft were obtained from the
5 ocean color group at Goddard Space Flight Center at http://oceancolor.gsfc.nasa.gov (McClain et al., 2004). The SeaStar spacecraft was launched in 1997 and SeaWiFS data are available from September 1997. The Level-3 mapped eight day data product was used here. This is provided on a resolution of 1/12° in both latitude and longitude, which corresponds to 9.2 km in latitude and 4.6 km in longitude at 60° N. These approx-
10 imately weekly averages were collocated with the $f\mathrm{CO}_2^{sw}$ data obtained on *Nuka* with a mean distance separation of 2.9 km spanning 0.04 to 5.2 km. The available chl *a* data covered the time period 17 March to 23 October 2005. Following Lévy et al. (2005), chl *a* values greater than 5 mg m^{-3} were considered unrealistically high and discarded, except for in the East Greenland Current region where much higher chl *a* concentra-
15 tions are known to occur (Holliday et al., 2006). This removed 193 of 21 806 collocated chl *a* observations.
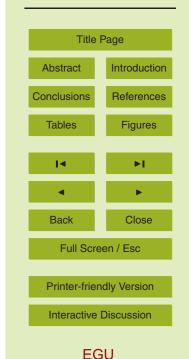
2.4 Ocean analysis data

The SSS and MLD estimates along the track of *Nuka* supplied by FOAM can be obtained at http://www.ncof.gov.uk/products.html (McCulloch et al., 2004). These data
20 are provided as daily fields on a 1/9° resolution, corresponding to 12.3 km in latitude and 6.2 km in longitude at 60° N. The ocean data assimilated by FOAM are obtained from a number of sources such as Argo profiling floats, XBT and CTD profiles, and AVHRR satellite-derived sea surface temperatures. The daily FOAM data were collocated with the *Nuka* $f\mathrm{CO}_2^{sw}$ data with a distance separation of between 0 and 7.8 km,
25 with a mean value of 4 km.

To evaluate of the reliability of the FOAM data, FOAM SST estimates were com-

EGU

pared with the temperatures measured at the seawater intake on *Nuka* (Fig. 4). This figure also includes a comparison between intake temperatures and SST data from the HYbrid Coordinate Ocean Model (HYCOM) ocean analysis product (Chassignet et al., 2007), which is provided on a daily basis at a resolution of 1/12° and obtainable from

[5] http://hycom.rsmas.miami.edu/index.shtml. The linear regression diagnostics are quite similar, with r^2 values of 0.92 and 0.89 for the FOAM and HYCOM data, respectively. The root mean square (rms) error is somewhat less for the HYCOM data, 0.70 compared to 0.82 for the FOAM data. However, whereas SST estimates from both HYCOM and FOAM compare well with the *Nuka* intake temperatures between 5 and 15°C, the

[10] HYCOM SST estimates tend to be a few degrees too cold at temperatures higher than 15°C, and around 5°C too warm at temperatures below 5°C. The HYCOM data thus appears too smooth, and in particular, the warm bias at low temperatures occurs in the westernmost regions, implying that HYCOM seems to have difficulties reproducing the conditions in the East Greenland Current. The error in the FOAM data is a lot less

[15] systematic. This was evaluated by regression analysis (not shown): HYCOM–intake temperature differences are highly correlated with intake temperature (slope: –0.3°C °C^{-1}; r^2: 0.6) whereas the FOAM–intake temperature differences are not (slope: – 0.04°C °C^{-1}; r^2: 0.02). Moreover, the FOAM SSS data is better correlated with the SSS data that were collected by the thermosalinograph (TSG) aboard *Nuka* (The TSG

[20] data are courtesy of Dr.Gilles Reverdin at LOCEAN/IPSL, Paris). In 2005, the TSG on *Nuka* collected data on 12 of the 27 crossings with $f\mathrm{CO_2^{sw}}$ data; FOAM data were preferred to get a complete dataset. Regression between FOAM SSS and TSG SSS yields a slope of 0.8, an intercept of 7.4 and an r^2 value of 0.88. The lower slope (0.44) and larger intercept (19.64) of the regression between HYCOM SSS and TSG SSS,

[25] which also has a lower r^2 (0.81), confirms that the HYCOM data are much smoother than the FOAM data. The FOAM ocean analysis data were therefore preferred.

2.5 Determination of the effect of processes controlling monthly changes of $f\mathrm{CO_2^{sw}}$

Since different processes may dominate in different areas we have divided the sampling area into four regions: the East Greenland Current, (EGC) defined as the region between 45° W where sampling was terminated or initiated at each crossing and east-

5 ward to the 2750 m isobath; the Irminger Basin (IrB), which extends from the 2750 m isobath and eastward to the top of the Reykjanes Ridge, but excluding shelf areas around Iceland with a depth cut-off at 500 m; the Iceland Basin (IcB) region, covering the area between the top of the Reykjanes Ridge and eastward to the European continental shelf at the 500 m isobath (this region includes the Hatton Plateau but excludes

10 shelf areas around Iceland and the Faeroes with a depth cut-off of 500 m); and the region to the east of the 500 m isobath at the European continental shelf edge is denoted the North Sea (NS).

The data were averaged for each region and each month, with each average $f\mathrm{CO_2^{sw}}$ value assumed to be representative of the 15th of each month. Given this, then for

15 each month, i, the change in $f\mathrm{CO_2^{sw}}$ was calculated as:

$$\Delta f\mathrm{CO_2^{sw,\textit{i}}} = \frac{f\mathrm{CO_2^{\textit{i}+1}} + f\mathrm{CO_2^{\textit{i}}}}{2} - \frac{f\mathrm{CO_2^{\textit{i}-1}} + f\mathrm{CO_2^{\textit{i}}}}{2} = \frac{f\mathrm{CO_2^{\textit{i}+1}} - f\mathrm{CO_2^{\textit{i}-1}}}{2} \quad (2)$$

First, the effect on $f\mathrm{CO_2^{sw}}$ from the change in temperature in each month was calculated as:

$$\Delta_T f\mathrm{CO_2^{\textit{i}}} = f\left(Ct_1^i, At_1^i, \mathrm{SSS}_1^i, \mathrm{SST}_1^{i+1}\right) - f\left(Ct_1^i, At_1^i, \mathrm{SSS}_1^i, \mathrm{SST}_1^i\right) \quad (3)$$

20 Where subscript "1" indicates the value of the first day in month i, determined as the mean of the average values in consecutive months:

$$X_1^i = \frac{X^i + X^{i-1}}{2} \quad (4)$$

All CO_2 system calculations were carried out using constants of Merbach et al. (1973) refit by Leuker et al. (2000) and the Matlab code provided by Zeebe and Wolf-Gladrow

EGU

(2001) at http://www.awi-bremerhaven.de/Carbon/co2book.html, but modified to work with CO_2 fugacity rather than partial pressure. The effects of phosphate and silicate were ignored. For the IrB and IcB regions At was estimated using the function derived by Lee et al. (2006), for the EGC we used the equation of Bellerby et al. (2005), and finally, for the NS the function At=21.533+1610 (A. Omar, personal communication) was employed. Mean Ct values for each month were determined from $f\text{CO}_2^{sw}$ and estimated At.

Second, and similar to Léfevre et al. (1994) and Lüger et al. (2004), the combined effects of mixing and biology on $f\text{CO}_2^{sw}$ were estimated from the monthly changes in nitrate. Decreasing values imply net community production, whereas increasing values imply net respiration and/or upwelling or horizontal transport of waters with remineralised organic matter:

$$\Delta_{MB}f\text{CO}_2^i = f(Ct_1^i + 7.2\Delta\text{NO}_3^i, At_1^i, \text{SSS}_1^i, \text{SST}_1^i) - f\left(Ct_1^i, At_1^i, \text{SSS}_1^i, \text{SST}_1^i\right) \tag{5}$$

where:

$$\Delta\text{NO}_3^i = \frac{\text{NO}_3^{i+1} + \text{NO}_3^i}{2} - \frac{\text{NO}_3^{i-1} + \text{NO}_3^i}{2} \tag{6}$$

The factor 7.2 in Eq. (5) is the ratio of carbon to nitrogen during remineralisation according to Körtzinger et al. (2001). Nitrate data were obtained from the World Ocean Atlas 2005 (Garcia et al., 2006)

Third, the effect of air-sea gas exchange was computed as:

$$\Delta_{AS}f\text{CO}_2^i = f(Ct_1^i + \Delta Ct_{AS}^i, At_1^i, \text{SSS}_1^i, \text{SST}_1^i) - f\left(Ct_1^i, At_1^i, \text{SSS}_1^i, \text{SST}_1^i\right) \tag{7}$$

where:

$$\Delta Ct_{AS}^i = \frac{d^i \times F^i}{mld^i} \tag{8}$$

Sea surface CO_2 fugacity in the subpolar North Atlantic

A. Olsen et al.

Where d^i is the number of days each month and F^i is the mean flux each month according to:

$$F^i = S^i k^i \left(f CO^i_{2,\text{atm}} - f CO^i_2 \right) \tag{9}$$

Mean solubility each month, S^i, was determined following Weiss (1974). Mean transfer velocity each month, k^i, was determined following Wanninkhof (1992):

$$k^i = 0.31 \times \left(\frac{\sum\limits_{j=1}^{n} U^2_{10,j}}{n} \right)^i \left(\frac{Sc^i}{660} \right)^{-\frac{1}{2}} \tag{10}$$

Where $U_{10,j}$ is 6 hourly wind speed data and n is the number of data in each region in each month i. The wind speeds were computed from the 6 hourly orthogonal velocity components at 10 m provided in the NCEP/NCAR reanalysis product (Kalnay et al., 1992).

Finally, the effect on $f CO_2$ of salinity changes was determined as

$$\Delta_{\text{SSS}} f CO^i_2 = f(Ct^i_1, At^i_1, SSS^i_1, SST^i_1) - f \left(Ct^i_1 \frac{sss^{i+1}_1}{sss^i_1}, At^i_1 \frac{sss^{i+1}_1}{sss^i_1}, SSS^{i+1}_1, SST^i_1 \right) \tag{11}$$

3 Results

3.1 Variation of $f CO^{sw}_2$ and related environmental parameters in 2005

Hovmöller diagrams of $f CO^{sw}_2$, $\Delta f CO_2$, SST, SSS, MLD, and chl a are shown in Figs. 5a–f. The background shading shows bottom depths. In particular, the untypical values encountered at 20° W in February were obtained on the Iceland Shelf (IcS) when the ship was on its way to a port call in Reykjavik.

All variables except SSS went through a pronounced seasonal cycle in 2005. The highest $f\mathrm{CO}_2^{sw}$ values, lowest SSTs and deepest MLDs were encountered from January through March. Waters over both the IcB and IrB were slightly supersaturated with respect to the atmospheric $f\mathrm{CO}_2$ level, and the NS and EGC were slightly undersatu-
5 rated. During this period, the warmest waters occurred over the IcB and were between 8 and 9°C. To the east of this moving into the NS temperatures dropped to around 6°C, and to the west crossing over the IrB and into the EGC temperatures decreased from around 7°C to less than 1°C.

In April 2005 the water started to heat up and the warming continued until August
10 and September. By that time the eastern NS temperatures had reached above 15°C, the IcB between 12 and 13°C, and the IrB was between 6 and 11°C depending on longitude. In the EGC the heating was much less pronounced.

This heating stratified the water column (Fig. 5e), which in turn initiated a phytoplankton bloom (Sverdrup, 1953) (Fig. 5f) which drew down the $f\mathrm{CO}_2^{sw}$ (Figs. 5a and b) as
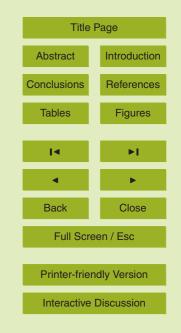15 quantified in the next section. The seasonal evolution in $f\mathrm{CO}_2^{sw}$ appears synchronous with that of both the MLD and chl a. In the IrB the MLD shoaled from several hundreds of meters and by June–August it reached only between 30 and 50 m. In this period surface chl a values were normally between 0.5 and 1 mg m^{-3} and the $f\mathrm{CO}_2^{sw}$ levels had decreased to between 320 and 340 μatm. The $f\mathrm{CO}_2^{sw}$ drawdown was larger in the
20 IcB, and values were less than 320 μatm; this appears coherent with the higher chl a concentrations and shallower MLD that occurred here compared to the IrB. As evaluated from the $f\mathrm{CO}_2^{sw}$ values, the bloom in the IcB appears to have progressed eastward and minimum values occurred at about 20° W in late June and at about 10° W in late July and early August. It is quite intriguing that a similar pattern is evident in the chl a
25 and MLD data: peak chl a concentrations were reached earlier toward the Reykjanes Ridge than toward the Hatton Trough, and the MLD was shallower to the west in early summer and to the east in late summer.

In the EGC, it appears as if the bloom peaked in May, with chl a concentrations exceeding 5 mg m^{-3} and $f\mathrm{CO}_2^{sw}$ values having decreased to less than 300 μatm, but

this is not certain as the succeeding ship tracks took a more southern route and data collection was stopped before the ship entered the shelf. This is most likely the reason for the increase in $f\mathrm{CO}_2^{sw}$ that appears to have occurred in June before low values were re-encountered in August and September.

⁵   In the NS the seasonal cycle in chl a is not as clear as in the other regions, and in the eastern regions of the NS concentrations were between 0.5 and 1 mg m^{-3} throughout the year. In the western regions of the NS chl a concentrations appear to have peaked twice, once in May–June and once in August–September. None of these features appear particularly coherent with the $f\mathrm{CO}_2^{sw}$ variability, which indicates that the bloom
¹⁰ progressed from east to west between April and July.

    By September the mixed layer started to deepen and surface waters became colder. No chl a data were available after late October, and by that time the concentration had dropped to between 0.25 and 0.5 mg m^{-3} and $f\mathrm{CO}_2^{sw}$ had increased to approximately 360 μatm. By December when data collection aboard *Nuka* ended for the year, $f\mathrm{CO}_2^{sw}$
¹⁵ was close to saturation with respect to the atmospheric concentration.

3.2   Analysis of factors controlling monthly changes of $f\mathrm{CO}_2^{sw}$

The results of the calculations described in Sect. 2.5 are displayed in Fig. 6; positive values indicate an increase in $f\mathrm{CO}_2^{sw}$. The upper row shows the monthly change in $f\mathrm{CO}_2^{sw}$ in each region. The residual changes shown in row 6 are quite substantial. We
²⁰ attribute this to the fact that we have employed nitrate values provided in the World Ocean Atlas 2005 (Garcia et al., 2006) in the calculations, since no sampling for nutrients was carried out aboard *Nuka*. Neither the magnitude nor timing of changes in the climatological nitrate data may be fully representative of the conditions in 2005. Nevertheless, we believe that Fig. 6 provides a decent summary of the importance of
²⁵ each $f\mathrm{CO}_2^{sw}$ driver in the different regions.

    The most dramatic $f\mathrm{CO}_2^{sw}$ change in 2005 occurred in the ECG in April when it decreased by almost 50 μatm, as can also be appreciated in the Hovmöller plot (Fig. 5a). The monthly changes in the IrB and IcB were not as large and came about later, reach-

ing nearly 30 μatm in May 2005. The cumulative drawdown in these two regions from March through June was only slightly larger than the drawdown in May in the EGC: 60 μatm in the IcB and 55 μatm in the IrB. In the NS the largest drawdown occurred in February, almost 30 μatm. In this region the $f\mathrm{CO}_2^{sw}$ seems to have been fairly stable from April through June 2005, with a consistent increase following in July. In the IcB, increasing values occurred one month later, in August, whereas the increase started in July in the IrB. As mentioned earlier we believe that the $f\mathrm{CO}_2^{sw}$ increase observed in June in the EGC is an artefact due to a southward change of the ship track, thus the autumn increase appears to have set in as late as October in 2005 in this region. It is also evident that the observed changes in $f\mathrm{CO}_2^{sw}$ in both the IrB and IcB follow those expected from mixing and biology, while the effects of temperature and gas exchange play a smaller role. Gas exchange is only important in summer and early fall when the air-sea CO_2 gradient is large and mixed layers are shallow. Changes in SSS do not have any significant effect on $f\mathrm{CO}_2^{sw}$ in any of the regions except for the NS. Here it seems to have induced significant decreases in $f\mathrm{CO}_2^{sw}$ during May and June. This may have resulted from a decrease in salinity due to increased runoff. Also, the salinities of inflowing Atlantic water are typically higher in winter than in summer (Lee et al., 1980). However, given the substantial spatial salinity gradients in the NS area (Fig. 1 and Lee et al., 1980) the effect can just as well be due to changes in the ship track. The air-sea flux had a larger effect on $f\mathrm{CO}_2^{sw}$ in the NS than in the IrB and IcB, because of the larger air-sea gradient and shallower mixed layers in the NS (Fig. 5). During the first half of the year it appears as if temperature had a larger effect on $f\mathrm{CO}_2^{sw}$ than biology and mixing in the NS.

In the EGC, biology and mixing appear to have dominated $f\mathrm{CO}_2^{sw}$ variations from February through May. No particular process stands out the rest of the year. Surprisingly and unlike any of the other regions, both temperature and biology and mixing appear to have reduced $f\mathrm{CO}_2^{sw}$ from August to October. This may very well reflect deficiencies in the WOA nitrate data.

3.3 Relationship between $f\mathrm{CO}_2^{sw}$ and temperature

Figure 7 presents wintertime (January–March) $f\mathrm{CO}_2^{sw}$ plotted as a function of SST in each of the regions introduced above, as well as on the IcS and the Faroe Bank (FB), defined by the 500 m isobath surrounding the islands. Regression diagnostics of the linear fits drawn in Fig. 7 are listed in Table 1, along with the number of observations and $f\mathrm{CO}_2^{sw}$ standard deviations for comparison with the rms values. The wintertime $f\mathrm{CO}_2^{sw}$ off the shelf regions in the subpolar North Atlantic is not related to temperature as evaluated from the *Nuka* 2005 data. In both the IcB and IrB, the winter $f\mathrm{CO}_2^{sw}$ was approximately 385 μatm (mean values of 384 and 386 μatm, respectively) over SSTs ranging from 4 to above 8°C. At temperatures higher than 8.5°C there is a slight tendency for $f\mathrm{CO}_2^{sw}$ to decrease with increasing temperatures.

In the shelf regions, $f\mathrm{CO}_2^{sw}$ generally shows distinct positive relationships with temperature. In the EGC, $f\mathrm{CO}_2^{sw}$ follows approximately the thermodynamic relationship of Takahashi et al. (1993), increasing by 3.8% °C^{-1} over the range of temperatures from −1 to 4.5 °C. This relationship is quite strong and explains 96% of the variability in $f\mathrm{CO}_2^{sw}$. On the IcS, the relationship between $f\mathrm{CO}_2^{sw}$ and temperature is slightly weaker and with a steeper slope, corresponding to 4.6% °C^{-1}. This is somewhat larger than the slope of the data obtained on the FB, which corresponds to 1.98% °C^{-1}. For all of the regions correct delineation is an issue. For instance, some of the data classified as IcS have the character of IrB data, and some of the data classified as IcB follow the FB trend. This is unavoidable, but it appears to be a truly serious issue only for the NS, where several temperature dependant relationships seem to exist. However, the data that define the most obvious relationship were acquired in March and the positions of these encompass the other data that were obtained in January and February, so the different slopes may reflect seasonal changes in the slope. Thus, in all shelf regions except in the NS, SST appears to be a fair predictor for $f\mathrm{CO}_2^{sw}$ in winter with rms values between 3.8 and 6 μatm. In the open ocean regions no predictor is required in winter, as $f\mathrm{CO}_2^{sw}$ appears stable over the whole range of temperatures with a variability of only

Title Page

Abstract | Introduction

Conclusions | References

Tables | Figures

◄ | ►

◄ | ►

Back | Close

Full Screen / Esc

Printer-friendly Version

Interactive Discussion

EGU

±3 μatm.

Throughout the rest of the year fCO$_2^{sw}$ is not related to temperature on the shelves. Linear regression gives r^2 values of 0.24, 0.13 and 0.01 for the EGC, FB, and NS, respectively. The corresponding annual relationships are poor, with r^2 values of 0.2, 0.14, and 0.01 and rms values of 46, 13.6, and 31.3 μatm, only slightly better than the variability in the data (51.5, 14.7, and 31.8 μatm). With regard to the IcS, non-winter data were only obtained in April, so an annual relationship was not evaluated.

In the open regions, i.e. the IrB and IcB, linear regression with SST explains roughly 50% of the fCO$_2^{sw}$ variability throughout 2005. Specifically, the r^2 and rms values for the annual regression in the IcB are 0.56 and 17 μatm, respectively, and 0.50 and 14 μatm in the IrB. The rms values can be compared with the standard deviation in the data: 25.5 μatm in the IcB and 19.6 μatm in the IrB. Since biology and mixing dominate seasonal fCO$_2^{sw}$ evolution the overall slope of each relationship is negative, with fCO$_2^{sw}$ decreasing as temperature increases (Fig. 8). Moreover, both relationships trace an elliptical shape and for any given temperature fCO$_2^{sw}$ is lower during spring and early summer than it is during late summer and fall. Similar hystereses have been observed in the North Atlantic subtropical gyre as well as in the Caribbean Sea and have been attributed to both gas exchange (Lefévre and Taylor, 2002) and surface salinity variations (Wanninkhof et al., 2007). For the regions discussed here the effect of salinity on fCO$_2^{sw}$ is negligible (Sect. 3.2). Gas exchange, on the other hand, acts to increase fCO$_2^{sw}$ over summer and so is the likely cause of the hysteresis in the subpolar North Atlantic.

Finally, the slopes of SST–fCO$_2^{sw}$ regressions are quite different from month to month. This more than anything else illustrates that equations derived from data obtained in some months will not in general reproduce fCO$_2^{sw}$ in others

3.4 Relationship between fCO$_2^{sw}$ and chlorophyll a

As with Lüger et al. (2004) and Nakoa et al. (2006), linear relationships between fCO$_2^{sw}$ and chl a could not be identified on an annual scale in any of the regions that we have

A. Olsen et al.

defined, but that does not exclude the existence of such relationships on smaller spatial and temporal scales as observed by Watson et al. (1991). However, exponential decay curves with a constant term reproduce $f\mathrm{CO}_2^{sw}$ quite well, particularly in the IrB and IcB as shown in Fig. 9 and Table 2. The data stem from March through October, the only time period for which SeaWiFS chl a data were available. The shape of the curves reflects the fact that as nutrients become exhausted in this region, primary production and chl a concentration are fuelled by regenerated rather than new nutrients. Moreover, as carbon concentration decreases the Revelle factor increases, and so a given change in Ct results in smaller $f\mathrm{CO}_2^{sw}$ changes.

The $f\mathrm{CO}_2^{sw}$ –chl a relationship is slightly weaker than the relationship with SST in the IcB and stronger than the SST relationship observed in the IrB, for which r^2 values of 0.56 and 0.50, respectively, were obtained (Sect. 3.3). However, this is partly due to the selection of different data. For a more accurate comparison, regressions with SST using the same data that were used for the chl a regressions yield r^2 values of 0.45 and 0.47 for the IcB and IrB. Thus chl a appears to be a better extrapolation parameter than SST in both regions. Moreover, the $f\mathrm{CO}_2^{sw}$ –chl a relationships are quite similar in the IrB and IcB, unlike the relationships between $f\mathrm{CO}_2^{sw}$ and SST. The single equation $f\mathrm{CO}_2^{sw}=324 + 86.82e^{-2.94(chl\,a)}$ adequately describes the $f\mathrm{CO}_2^{sw}$ –chl a relationship in the IrB and IcB combined, with $r^2=0.57$ and rms=14.5 μatm. For comparison, the equation describing the $f\mathrm{CO}_2^{sw}$–SST relationship in these combined regions, using only data that are employed in the chl a relationship yields an r^2 value of 0.46 and a rms of 16.1 μatm. There is, however, some variation in the accuracy of the chl a relationships with season. As illustrated in Fig. 10a the chl a relationships do not fully reproduce the seasonal amplitude in $f\mathrm{CO}_2^{sw}$ and tend to underestimate high $f\mathrm{CO}_2^{sw}$ values and overestimate low ones. This tendency is slightly stronger in the IcB than in the IrB.

In the shelf regions, the relationships between $f\mathrm{CO}_2^{sw}$ and chl a (Table 2) are much stronger than the relationships between $f\mathrm{CO}_2^{sw}$ and SST , and using only data where chl a are available for linear regression between $f\mathrm{CO}_2^{sw}$ and SST yields r^2 values of

1754

0.18 for the EGC, 0.32 for the IcS, 0.22 for the FB, and 0.01 for the NS. As in the IcB and IrB, the relationship with chl a tends to underestimate high and overestimate low $f\mathrm{CO}_2^{sw}$ values in these regions as well (not shown).

3.5 Relationship between $f\mathrm{CO}_2^{sw}$ and mixed layer depth

Subpolar North Atlantic $f\mathrm{CO}_2^{sw}$ values are related to MLD through exponential growth curves as illustrated in Fig. 11 and summarised in Table 3. The shape of the relationships reflects a linear relationship between $f\mathrm{CO}_2^{sw}$ and MLD from the commencement of the bloom until the MLD deepening during fall, and the stabilisation of $f\mathrm{CO}_2^{sw}$ at wintertime values which are unrelated to MLD.

As can be appreciated from Fig. 10b the MLD relationships reproduce the seasonal amplitude in $f\mathrm{CO}_2^{sw}$ better than the chl a relationships. In the IrB, no particular bias appears in any of the seasons. In the IcB there is a negative bias of approximately 5 μatm in winter, otherwise the estimates are accurate. In the IcB, the $f\mathrm{CO}_2^{sw}$–MLD relationship explains 81% of the variability in $f\mathrm{CO}_2^{sw}$; in the IrB, 77%. On it's own, MLD can reproduce $f\mathrm{CO}_2^{sw}$ to better than ±10 μatm in the IrB and ±12 μatm in the IcB on an annual basis. This is approximately the accuracy required to estimate the northern North Atlantic annual sink size to within 0.1 Gt yr^{-1} (Sweeney et al., 2002). In these regions, MLD is a better $f\mathrm{CO}_2^{sw}$ extrapolation parameter than both SST and chl a. For a more specific comparison, regression with MLD using only data with chl a observations yields r^2 values of 0.68 (IcB) and 0.72 (IrB), which are better than the regressions with chl a for the same data (Table 2). A specific analysis is not required for SST, since all data have both SST and MLD. The relationships are quite similar in the IcB and IrB, and the single equation $f\mathrm{CO}_2^{sw} = 439.89 - 252.46e^{-0.245\mathrm{MLD}}$ reproduces $f\mathrm{CO}_2^{sw}$ in these regions combined to within ±12.2 μatm with an r^2 value of 0.75.

On the shelves, MLD regressions are not as good, in particular in the EGC where an exponential growth curve fails to reproduce $f\mathrm{CO}_2^{sw}$ variability. On the IcS, $f\mathrm{CO}_2^{sw}$ is essentially unrelated to MLD; the poor fit is probably the result of the lack of data from the full annual cycle. Only January through April was sampled in this region. Of the fits

Sea surface CO$_2$ fugacity in the subpolar North Atlantic

A. Olsen et al.

EGU

on the FB and in the NS, the former is better and explains 46% of the variability, which is similar to the chl a regression. In the NS, the relationship with MLD is better than the relationship with chl a, but it can only estimate $f\text{CO}_2^{sw}$ to within $\pm 26\,\mu$atm.

4 Summary and further remarks

The data collected aboard *Nuka Arctica* in 2005 have given an unprecedented view of annual surface ocean $f\text{CO}_2$ variability in the subpolar North Atlantic. Excluding the shelf areas, the $f\text{CO}_2^{sw}$ was in equilibrium with the atmospheric concentration in winter. Throughout summer it was reduced by approximately 60 μatm, the net result of a biological drawdown of CO_2 that was not fully counteracted by the increase in temperature and uptake of CO_2 from the atmosphere. In fall the dominating processes were mixing and gas exchange which resulted in an $f\text{CO}_2^{sw}$ increase. These mechanisms give rise to a negative correlation between $f\text{CO}_2^{sw}$ and SST in this region. In addition, there was a considerable hysteresis due to the uptake of atmospheric CO_2 in late summer and fall. This hysteresis and the fact that $f\text{CO}_2^{sw}$ was unrelated to SST in winter makes SST a poor $f\text{CO}_2^{sw}$ extrapolation parameter in the IcB and IrB.

Given the reliance of $f\text{CO}_2^{sw}$ on biology and mixing, and the reliance of biology on mixing (Sverdrup, 1954), the relationship observed between $f\text{CO}_2^{sw}$ and MLD is not unexpected. The relationship followed approximately an exponential growth curve, the combination of a linear relationship during spring, summer and fall, and $f\text{CO}_2^{sw}$ being constant as MLD exceeded 300 m, typical during winter. By itself MLD reproduced $f\text{CO}_2^{sw}$ to within $\pm 10\,\mu$atm in the IrB and $\pm 12\,\mu$atm in the IcB.

In contrast to other studies (Lüger et al., 2004; Watson et al., 1991; Nakaoa et al., 2006) we have been able to identify basin-wide relationships between $f\text{CO}_2^{sw}$ and chl a, valid on nearly annual time scales. An exponential decay curve describes the relationship with an accuracy of 15.6 μatm in the IcB and 10.4 μatm in the IrB. The predictive capability of chl a alone in the subpolar Atlantic is better than that of relationships in the Pacific Ocean that utilized both SST and chl a (Ono et al., 2004). We believe that the

Sea surface CO_2 fugacity in the subpolar North Atlantic

A. Olsen et al.

Title Page

Abstract | Introduction

Conclusions | References

Tables | Figures

◀ | ▶

◀ | ▶

Back | Close

Full Screen / Esc

Printer-friendly Version

Interactive Discussion

EGU

shape of the curve reflects the fact that new production is limited by nutrient availability during summer. Similar curves should be tested in other regions as well.

In order to quantify the North Atlantic CO_2 sink size to within $0.1\,Gt\,yr^{-1}$, fCO_2^{sw} should be mapped with an accuracy of $10\,\mu atm$ (Sweeney et al., 2002). Given the relationships identified here this seems to be within reach and will be further explored by Chierici et al. (in prep.).

On the shelves annual regressions were in general not as good as in the IcB and IrB, and we believe this reflects issues with delineation (in particular for the NS), seasonal changes in slopes, insufficient data coverage, and more heterogeneous hydrographic conditions. Dedicated studies should address these regions.

Finally, we would like to note that the data obtained on *Nuka* shows that the air-sea fCO_2 difference in the region was quite small during the winter of 2005 and the region does not at all appear to have been a strong CO_2 sink in this season, but rather a small source. This lends support to the conclusion of Perez et al. (2002), who unlike Gruber et al. (1996) found that the air-sea disequilibrium in total carbon in this region must be quite small during the time of water mass formation, which is winter. The disequilibrium estimates of Gruber et al. (1996) were comparable to those of Takahashi et al. (1995) showing undersaturation of more than $30\,\mu atm$ in winter in the region. A comparison of the *Nuka* 2005 data with the more recent Takahashi et al. (2002) climatology revealed a difference in saturation levels of $20\pm26\,\mu atm$ (annual average with one standard deviation), with the climatology data being the most undersaturated (not shown). Several factors, most likely in combination, may have contributed to this difference: the assumption of no secular fCO_2^{sw} trends used when collapsing several years of data on to a 1995 climatology, lack of data over the whole region throughout the year, and finally a large increase in fCO_2^{sw} (Lefévre et al., 2004, Olsen et al., 2006, Omar and Olsen, 2006, Corbiere et al., 2007). To improve this situation the 2005 *Nuka* data have been submitted for inclusion in the next climatology of Takahashi et al. (2007)[2]. In this context it is interesting to note that Takahashi et al. (1993) observed

---

[2]Takahashi, T., Sutherland, S., Wanninkhof, R., et al.: Climatological Mean and Decadal

Sea surface CO_2 fugacity in the subpolar North Atlantic

A. Olsen et al.

that the air-sea disequilibrium was very small and slightly positive at 63° N, 20° W in the 1980s. Given the *Nuka* data from 2005 this situation appears unchanged, implying that the fCO$_2$ growth rate in the atmosphere and the ocean must have been the same. This is in contrast to Corbiere et al. (2007) and Lefévre et al. (2004), who both observed
5 oceanic growth rates larger than the atmospheric. It is, however, reconcilable with the lower end of the range of growth rate estimates presented by Omar and Olsen (2006), between 1.5 and 3 μatm yr^{-1}. More than anything else this illustrates that there are large uncertainties in current knowledge on the secular trends in fCO$_2^{sw}$ in this region. A sustained surface observation program is essential if we are to fully understand ocean
10 carbon system response to anthropogenic emissions.

References

Bellerby, R. G. J., Olsen, A., Furevik, T., and Anderson, L. G.: Response of the surface ocean CO$_2$ system in the Nordic Seas and northern North Atlantic to climate change, in The Nordic
25 Seas: An Integrated Perspective, edited by: Drange, H., Dokken, T., Furevik, T., Gerdes, R., and Berger, W., Geophys. Monogr. Ser., 158, 189–197, AGU, Washington D.C., 2005.

Change in Surface Ocean pCO2 and Net Sea-air CO$_2$ flux over the Global Oceans, Deep-Sea Res., in preparation, 2007.

Sea surface CO$_2$ fugacity in the subpolar North Atlantic

A. Olsen et al.

Title Page

Abstract	Introduction
Conclusions	References
Tables	Figures

◀ | ▶

◀ | ▶

Back | Close

Full Screen / Esc

Printer-friendly Version

Interactive Discussion

EGU

Boutin, J., Etcheto, J., Dandonneau, Y., Bakker, D. C. E., Feely, R. A., Inoue, H. Y., Ishii, M., Ling, R. D., Nightingale, P. D., Metzl, N., and Wanninkhof, R.: Satellite sea surface temperature: A powerful tool for interpreting in situ pCO_2 in the equatorial Pacific Ocean, Tellus B, 51, 490–508, 1999.

Chassignet, E. P, Hurlburt, H. E., Smedstad, O. M., Halliwell, G. R., Hogan, P. J., Wallcraft, A. J., Baraille, R., and Bleck, R.: The HYCOM (Hybrid Coordinate Ocean Model) data assimilative system, J. Marine Syst., 65, 60–83, 2007.

Chierici, M., Fransson, A., and Nojiri, Y.: Biogeochemical processes as drives of surface fCO_2 in constrasting provinces in the North Pacific Ocean, Global Biogeochem. Cycles, 20, GB1009, doi:10.1029/2004GB002356, 2006.

Cooper, D. J., Watson, A. J., and Ling, R. D.: Variation of pCO_2 along a North Atlantic shipping route (U.K. to the Caribbean): A year of automated observations, Mar. Chem., 72, 151–169, 1998.

Corbiere, A., Metzl, N., Reverdin, G., Brunet, C., and Takahashi, T.: Interannual and decadal variability of the oceanic carbon sink in the North Atlantic subpolar gyre, Tellus B, 59, 168–178, 2007.

Cosca, C. E., Feely, R. A., Boutin, J., Etcheto, J., McPhaden, M. J., Chavez, F. P., and Strutton, P. G.: Seasonal and interannual CO_2 fluxes for the central and eastern equatorial Pacific Ocean as determined from fCO_2-SST relationships, J. Geophys. Res, 108, 3278, doi:10.1029/2000JC000677, 2003.

Feely, R. A., Wanninkhof, R., Milburn, H. B., Cosca, C. E., Stapp, M., and Murphy, P. P.: A new automated underway system for making high precision pCO_2 measurements onboard research ships, Anal. Chim. Acta, 377, 185–191, 1998.
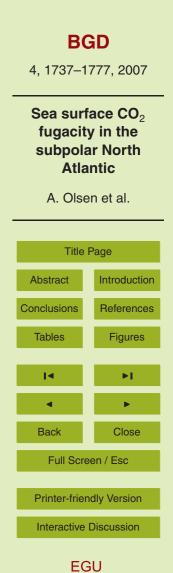
Frantantoni, D. M.: North Atlantic surface circulation during the 1990's observed with satellite-tracked drifters, J. Geophys. Res., 106, 22 067–22 093, 2001.

Garcia, H. E., Locarnini, R. A., Boyer, T. P., and Antonov, J. I.: World Ocean Atlas 2005, Volume 4: Nutrients (phosphate, nitrate, silicate), edited by S. Levitus, NOAA Atlas NESIDS 64, U.S Government Printing Office, Washington D.C., 396 pp, 2006.

Gruber, N., Sarmiento, J. L., and Stocker, T. F.: An improved method for detecting anthropogenic CO_2 in the oceans, Global Biogeochem. Cycles, 10, 809–837, 1996.

Hansen, B. and Østerhus, S.: North Atlantic-Nordic Seas exchanges, Prog. Oceanogr., 45, 109–208, 2000.

Holliday, N. P., Waniek, J. J., Davidson, R., Wilson, D., Brown, L., Sanders, R., Pollard, R. T.,

Title Page

Abstract | Introduction

Conclusions | References

Tables | Figures

◄ | ►|

◄ | ►

Back | Close

Full Screen / Esc

Printer-friendly Version

Interactive Discussion

and Allen, J. T.: Large-scale physical controls on phytoplankton growth in the Irminger Sea Part I: Hydrographic zones, mixing and stratification, J. Marine Syst., 59, 201–218, 2006.

Kalnay, E., Kanamitsu, M., Kistler, R., Collins, W., Deaven, D., Gandin, L., Iredell, M., Saha, S., White, G., Woollen, J., Zhu, Y., Chelliah, M., Ebisuzaki, W., Higgins, W., Janowiak, J., Mo, K. C., Ropelewski, C., Leetmaa, A., Reynolds, R., and Jenne, R.: The NCEP/NCAR Reanalysis Project, B. Am. Meteorol. Soc., 77, 437–471, 1996.

Körtzinger, A., Hedges, J. I., and Quay, P. D.: Redfield ratios revisited: Removing the biasing effect of anthropogenic CO_2, Limnol. Oceanogr., 46, 964–970, 2001.

Lacan, F. and Jeandel, C.: Subpolar Mode Water formation traced by neodynium isotopic composition, Geophys. Res. Lett., 31, L14306, doi:10.1029/2004GL019747, 2004.

Lee, A.J.: North Sea: Physical Oceanography, in: The North-West European shelf seas: the sea bed and the sea in motion, part II physical and chemical oceanography and chemical resources, edited by: Banner, F. T., Collins, M. B., and Massie, K. S., Elsevier Oceanography Series 24b, 467–493, 1980.

Lee, K., Tong, L. T., Millero, F. J., Sabine, C. L., Dickson, A. G., Goyet, C., Park, G.-H., Wanninkhof, R., Feely, R. A., and Key, R. M.: Global relationships of total alkalinity with salinity and temperature in surface waters of the world's oceans, Geophys. Res. Lett., 33, L19605, doi:10.1029/2006GL027207, 2006.

Lefévre, N., Watson, A. J., Olsen, A., Rios, A. F., Perez, F. F., and Johannessen, T.: A decrease in the sink for atmospheric CO_2 in the North Atlantic, Geophys. Res. Lett., 31, L07306, doi:10.1029/2003GL018957, 2004.

Lefévre, N. and Taylor, A.: Estimating pCO_2 from sea surface temperatures in the Atlantic gyres, Deep-Sea Res. I, 49, 539–554, 2002.

Lefévre, N., Andrié, C., and Dandonneau, Y.: pCO_2, chemical properties, and estimated new production in the Equatorial Pacific in January – March 1991, J. Geophys. Res., 99, 12 639–12 654, 1994.

Lévy, M., Lehan, Y., André, J.-M., Mémery, L., Loisel, H., and Heifetz, E.: Production regimes in the northeast Atlantic: A study based on Sea-viewing Wide Field of view Sensor (SeaWiFS) chlorophyll and ocean general circulation model mixed layer depth, J. Geophys. Res., 110, C07S10, doi:10.1029/2004JC002771, 2005.

Lueker, T. J., Dickson, A. G., and Keeling, C. D.: Ocean pCO_2 calculated from dissolved inorganic carbon, alkalinity and equations for K_1 and K_2: validation based on laboratory measurements of CO_2 in gas and seawater at equilibrium, Mar. Chem., 70, 105–119, 2000.

Sea surface CO_2 fugacity in the subpolar North Atlantic

A. Olsen et al.

Lüger, H., Wallace, D. W. R., Körtzinger, A., and Nojiri, Y.: The pCO_2 variability in the midlatitude North Atlantic Ocean during a full annual cycle, Global Biogeochem. Cycles, 18, GB3023, doi:10.1029/2003GB002200, 2004.

McCartney, M. S. and Talley, L. D.: The Subpolar Mode Waters of the North Atlantic Ocean, J. Phys. Oceanogr., 12, 1169–1188, 1982.

McClain, C. R., Feldmann, G. C., and Hooker, S. B.: An overview of the SeaWiFS project and strategies for producing climate research quality global ocean bio-optical time series, Deep-Sea Res. II, 51, 5–42, 2004.

McCulloch, M. E., Alves, J. O. S., and Bell, M. J.: Modelling shallow mixed layers in the north-east Atlantic, J. Mar. Syst., 52, 107–119, 2004.

Merbach, C., Culberson, C. H., Hawley, J. E., and Pytkowicz, R. M.: Measurement of apparent dissociation contants of carbonic acid in seawater at atmospheric pressure, Limnol. Oceanogr., 18, 533–541, 1973.

Nakaoa, S. I., Aoki, A., Nakazawa, T., Hashida, G., Morimoto, S., Yamanouchi, T., and Yoshikawa-Inoue, H.: Temporal and spatial variations of the oceanic pCO_2 and air- sea CO_2 flux in the Greenland Sea and Barents Sea, Tellus B, 58, 148–161, 2006.

Nelson, N. B., Bates, N. R., Siegel, D. A., and Michaels, A. F.: Spatial variability of the CO_2 sink in the Sargasso Sea, Deep-Sea Res. II, 48, 1801–1821, 2001.

Olsen A., Omar, A. M., Bellerby, R. G. J., Johannessen, T., Ninnemann, U., Brown, K. R., Olsson, K. A., Olafsson, J., Nondal, G., Kivimäe, C., Kringstad, S., Neill, C., and, Olafsdottir, S.: Magnitude and origin of the anthropogenic CO_2 increase and ^{13}C Suess effecct in the Nordic Seas since 1981, Global Biogeochem. Cycles, 20, GB3027, doi:10.1029/2005GB002669, 2006.

Olsen, A., Triñanes, J. A., and Wanninkhof, R.: Sea-air flux of CO_2 in the Caribbean Sea estimated using in situ and remote sensing data, Remote Sens. Environ., 89, 309–325, 2004.

Olsen, A., Bellerby, R. G. J., Johannessen, T., Omar, A. M., and Skjelvan, I.: Interannual variability in the wintertime air-sea flux of carbon dioxide in the northern North Atlantic, 1981–2003. Deep-Sea Res. I, 50, 1323–1338, 2003.

Omar, A. M. and Olsen, A.: Reconstructing the time history of the air-sea CO_2 disequilibrium and its rate of change in the eastern subpolar North Atlantic, 1972-1989, Geophys. Res. Lett., 33, L04602, doi:10.1029/2005GL025425, 2006.

Ono, T., Saino, T., Kurita, N., and Sasaki, K.: Basin-scale extrapolation of shipboard pCO_2 data

Sea surface CO_2 fugacity in the subpolar North Atlantic

A. Olsen et al.

by using satellite SST and Chla, Int. J. Remote Sens., 25, 3803–3815, 2004.

Orvik, K. A. and Niiler, P.: Major pathways of Atlantic water in the northern North Atlantic and Nordic Seas toward Arctic, Geophys. Res. Lett., 29(19), 1896, doi:10.1029/2002GL015002, 2002.

5 Pérez, F. F, Álvarez, M., and Rios, A. F.: Improvements on the back-calculation technique for estimating anthropogenic CO_2, Deep-Sea Res. I, 49, 859–875, 2002.

Pollard, R. T., Read, J. F., Holiday, N. P., and Leach, H.: Water Masses and circulation pathways through the Iceland Basin during Vivaldi 1996, J. Geophys. Res., 109, C04004, doi:10.1029/2003JC002067, 2004.

10 Prentice, I. C., Farquhar, G. D., Fasham, M. J. R., Goulden, M. L., Heimann, M., Jaramillo, V. J., Kheshgi, H. S., Ke Quéré, C., Scholes, R., and Wallace, D. W. R.:The Carbon Cycle and Atmospheric Carbon Dioxide, in Climate Change 2001: The Scientific Basis, Contribution of Working Group I to the Third Assessment Report of the Intergovernmental Panel on Climate Change, edited by: Houghton, J. T., Ding, Y., Griggs, D. J., Noguer, M., van der Linden, P.
15 J., Dai, X., Maskell, K., and Johnson, C.A., Cambridge University Press, Cambridge, United Kingdom and New York, NY, USA, 881 pp, 2001.

Reverdin, G., Niiler, P. P., and Valdimirsson, H.: North Atlantic Surface Currents, J. Geophys. Res., 108(C1), 3002, doi:10.1029/2001JC001020, 2003.

Stephens, M. P., Samuels, G., Olson, D. B., Fine, R. A., and Takahashi, T.: Sea-air flux of CO_2 in
20 the North Pacific using shipboard and satellite data, J. Geophys. Res., 100, 13 571–13 583, 1995.

Sverdrup, H. U.: On conditions for the vernal blooming of phytoplankton, J. Conc. Int. P. Exp. de la Mer, 18, 287-295, 1953.

Sweeney, C., Takahashi, T., and Gnanadesikan, A.: Spatial and temporal variability of surface
25 water pCO_2 and sampling strategies. pp. 155-175 in: A large-scale CO_2 observing plan: In situ oceans and atmosphere, edited by: Bender, M., Doney, S., Feely, R., et al. , National Technical Information Service, Springfield, Virginia, USA, 2002.

Takahashi, T., Sutherland, S. C, Sweeney, C., Poisson, A., Metzel, N., Tilbrook, B., Bates, N., Wanninkhof, R., Feely, R. A., Sabine, C., Olafsson, J., and Nojiri,Y.: Global sea-air CO_2
30 flux based on climatological ocean pCO_2 and seasonal biological and temperature effects, Deep-Sea Res. II, 1601–1622, 2002.

Takahashi, T., Takahashi, T. T., and Sutherland, S. C.: An assessment of the role of the North Atlantic as a CO_2 sink, Phil. Trans. R. Soc., London, B, 348, 143–152, 1995.

Sea surface CO_2 fugacity in the subpolar North Atlantic

A. Olsen et al.

EGU

Takahashi, T., Olafsson, J., Goddard, J. G., Chipman, D. W., and Sutherland, S. C.: Seasonal variation of CO_2 and nutrients in the high-latitude surface oceans: a comparative study, Global Biogeochem. Cycles., 7, 843–878, 1993.

Wallace, D. W. R.: Storage and transport of excess CO_2 in the oceans: The JGOFS/WOCE global CO_2 survey, in: Ocean Circulation and Climate: Observing and Modelling the Global Ocean, edited by: Siedler, G., Church, J., and Gould, J., Elsevier, New York, 489–521, 2001.

Wanninkhof, R., Olsen, A., and Triñanes, J.: Air-sea CO_2 fluxes in the Caribbean Sea from 2002-2004, J. Mar. Syst., 66, 272–284, 2007.

Wanninkhof, R. and Thoning, K.: Measurement of fugacity of CO_2 in surface water using continuous and discrete sampling methods, Mar. Chem., 44, 189–201, 1993.

Wanninkhof, R.: Relationship Between Wind Speed and Gas Exchange Over the Ocean, J. Geophys. Res., 97, 7373–7382, 1992.

Watson, A. J., Robinson, C., Robertson, J. E., Williams, P. J. le B., and Fasham, M. J. R.: Spatial variability in the sink for atmospheric carbon dioxide in the North Atlantic, Nature, 350, 50–53, 1991.

Weiss, R. F.: Carbon dioxide in water and seawater: The solubility of a nonideal gas, Mar. Chem., 2, 201–215, 1974.

Weiss, R. and Price, B. A.: Nitrous oxide solubility in water and seawater, Mar. Chem., 8, 347–359, 1980.

Zeebe, R. and Wolf-Gladrov, D.: CO_2 in seawater: equilibrium, kinetics, isotopes, Elsevier Oceanography Series 65, Elsevier, Amsterdam, 346 pp, 2001.
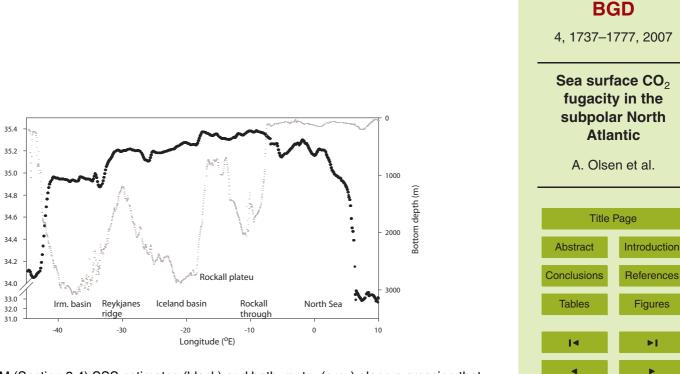
Sea surface CO_2 fugacity in the subpolar North Atlantic

A. Olsen et al.

Title Page

Abstract	Introduction
Conclusions	References
Tables	Figures

◀ | ▶|

◀ | ▶

Back | Close

Full Screen / Esc

Printer-friendly Version

Interactive Discussion

EGU

Table 1. Regression diagnostics for the relationship $f\mathrm{CO}_2^{sw}$=a*SST+b in the different regions during winter (January–March).

Region	a	b	r^2	rms	stdev. in data	n
IcB	−0.373	387.64	0.0024	3.90	3.91	2388
IrB	0.694	381.67	0.0080	2.47	2.58	1906
EGC	13.0	317.98	0.96	5.65	27.3	670
IcS	17.3	263.05	0.83	6.05	14.7	704
FB	7.08	320.02	0.45	3.80	5.12	482
NS	18.0	225.81	0.67	22.2	38.4	3042

EGU

Table 2. Diagnostics for the equation $f\mathrm{CO}_2^{sw}=a+b*e^{-c(\mathrm{chl}\,a)}$ for the different regions from March–October.

Region	a	b	c	r^2	rms	stdev. in data	n
IcB	322.92	84.92	3.01	0.52	15.6	22.4	7295
IrB	334.13	91.54	3.77	0.70	10.4	19.1	3917
EGC	234.47	160.3	1.43	0.49	40.6	56.6	2283
IcS	370.81	22.05	1.03	0.44	5.05	6.74	355
FB	321.32	61.59	1.09	0.48	11.2	15.5	567
NS	293.45	63.36	0.81	0.21	24.4	27.4	7191

EGU

Table 3. Diagnostics used for the equation $f\mathrm{CO}_2^{\mathrm{sw}}=a\text{-}b*e^{-c\mathrm{MLD}}$ for the different regions on an annual basis.

Region	a	b	c	r^2	rms	stdev. in data	n
IcB	381.54	88.84	0.014	0.81	11.3	25.6	16693
IrB	384.60	56.26	0.0086	0.77	9.45	19.6	9007
EGC	482.58	179.89	0.00060	0.12	48.2	51.3	3974
IcS	377.72	1.109×10^8	2.0×10^3	0.00	13.1	13.1	900
FB	368.81	94.56	0.042	0.46	12.0	16.2	857
NS	387.42	81.30	0.012	0.32	26.0	31.5	13952

EGU

Fig. 1. FOAM (Section 2.4) SSS estimates (black) and bathymetry (grey) along a crossing that took place during 2–6 April 2005. The specific cruise track is shown in Fig. 2.

Fig. 2. The ship track from 2-6 April 2005 and main features of the surface circulation inspired by McCartney and Talley (1982), Hansen and Østerhus (2000), Frantantoni (2001), Orvik and Niiler (2002), and Reverdin et al. (2003). The scaling of the arrows is by no means exact. Isobaths have been drawn at the 2000 and 1000 m depth levels.

Fig. 3. *Nuka Arctica f* CO$_2^{sw}$ sampling positions during 2005. Grey lines show isobaths at 3500, 2500, 1500 and 500 m. The heavy grey lines show the approximate borders of the regions: East Greenland Current (EGC), Irminger Basin (IrB), Iceland Basin (IcB), North Sea (NS), Iceland Shelf (IcS), and Faroe Bank (FB) defined in the text (Sects. 2.5, 3.1 and 3.3).
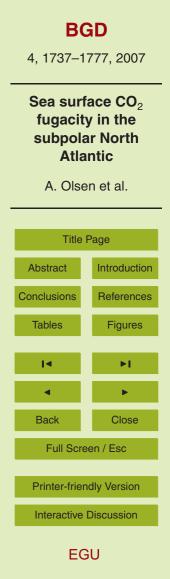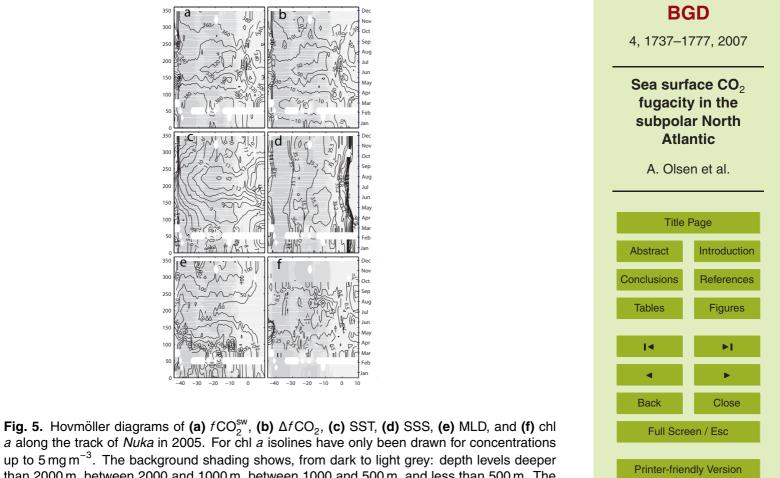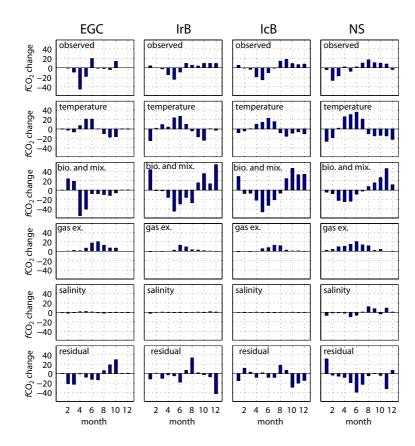
Title Page

Abstract   Introduction

Conclusions   References

Tables   Figures

◄◄   ►►

◄   ►

Back   Close

Full Screen / Esc

Printer-friendly Version

Interactive Discussion

Fig. 4. FOAM (grey) and HYCOM (black) SST estimates vs. intake temperatures from *Nuka*. The solid black line shows the 1:1 relationship.
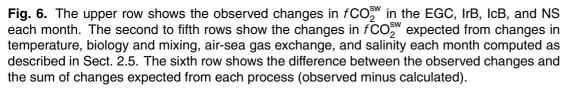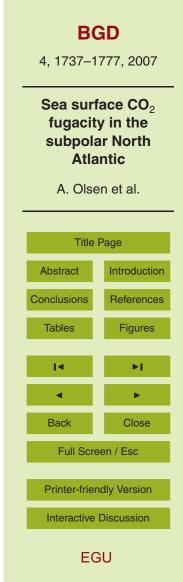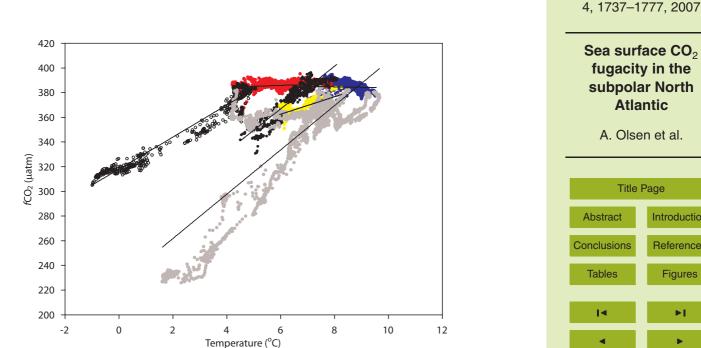
Fig. 5. Hovmöller diagrams of **(a)** fCO$_2^{sw}$, **(b)** ΔfCO$_2$, **(c)** SST, **(d)** SSS, **(e)** MLD, and **(f)** chl a along the track of *Nuka* in 2005. For chl a isolines have only been drawn for concentrations up to 5 mg m^{-3}. The background shading shows, from dark to light grey: depth levels deeper than 2000 m, between 2000 and 1000 m, between 1000 and 500 m, and less than 500 m. The positions of the data are shown with white lines. On some occasions missing data prevented sensible gridding; these regions have been left blank.

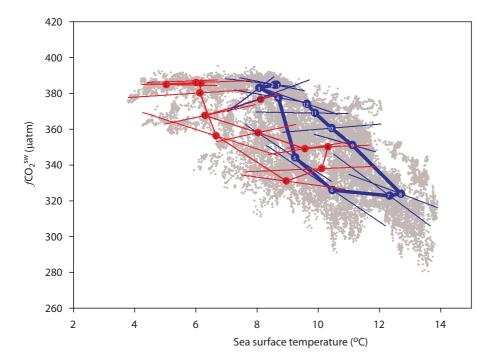**Fig. 6.** The upper row shows the observed changes in $f\mathrm{CO_2^{sw}}$ in the EGC, IrB, IcB, and NS each month. The second to fifth rows show the changes in $f\mathrm{CO_2^{sw}}$ expected from changes in temperature, biology and mixing, air-sea gas exchange, and salinity each month computed as described in Sect. 2.5. The sixth row shows the difference between the observed changes and the sum of changes expected from each process (observed minus calculated).

Fig. 7. Relationship between $f\mathrm{CO}_2^{sw}$ and SST during winter (January-March) in the EGC (open), IrB (red), IcB (blue), NS (grey), FB (yellow) and IcS (black). The black lines show the linear regressions for each region.

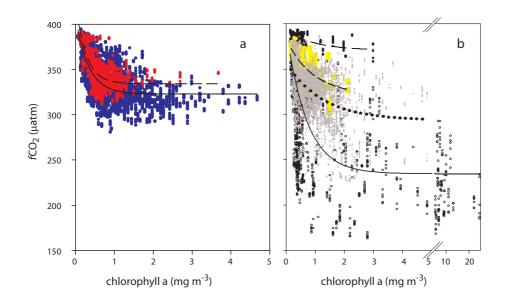**Fig. 8.** Annual relationships between $f\mathrm{CO}_2^{\mathrm{sw}}$ and SST in the IcB and IrB. The numbered circles represent the monthly mean values (red is IrB and blue is IcB) with the thin lines being the slopes of the linear regressions for each month.
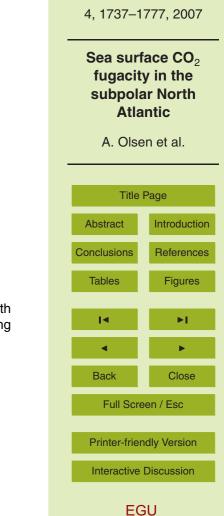
Fig. 9. Relationship between $f\text{CO}_2^{\text{sw}}$ and chl a in **(a)** the IcB (blue) and IrB (red) and **(b)** in the EGC (open), on the IcS (black) and FB (yellow), and in the NS (grey) from March-October. Note the break at $5\,\text{mg}\,\text{m}^{-3}$ at the chl a axis in (b). In (a) the solid and dashed lines show the regressions in the IcB and IrB, respectively. In (b) regressions are shown as follows: EGC: solid, IcS: long dash, FB: short dash, and NS: dotted.
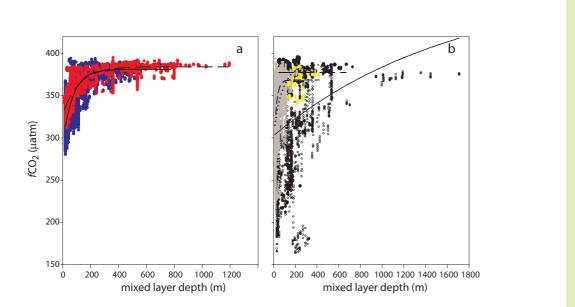
Fig. 10. Monthly mean observed (solid lines with solid circles) and predicted (dashed lines with open circles) $f\mathrm{CO}_2^{sw}$ in the IcB (black) and IrB (grey). In panel **(a)** $f\mathrm{CO}_2^{sw}$ was computed using the chl a dependencies (Table 2), in **(b)** using the MLD dependencies (Table 3).

Fig. 11. Annual relationships between $f\mathrm{CO_2^{sw}}$ and MLD in **(a)** the IcB (blue) and IrB (red) and **(b)** in the EGC (open), on the IcS (black) and FB (yellow), and in the NS (grey). In (a) the solid and dashed lines show regressions in the IcB and IrB, respectively. In (b) regressions are shown as follows: EGC: solid, IcS: long dash, FB: short dash, and NS: dotted.

EGU